BOREAS An international journal of Quaternary research

^{10}Be dating of the Main Terrace level in the Amblève valley (Ardennes, Belgium): New age constraint on the archaeological and palaeontological filling of the Belle-Roche palaeokarst

Journal:	*Boreas*
Manuscript ID:	BOR-024-2013.R1
Manuscript Type:	Original Article
Date Submitted by the Author:	n/a
Complete List of Authors:	Rixhon, Gilles; University of Cologne, Institute for Geography, Zülpicher Str. 45, 50674 Bourlès, Didier; CEREGE, UMR 7330 Aix Marseille Université-CNRS, Technopôle Méditerranéen de l'Arbois, Braucher, Régis; CEREGE, UMR 7330 Aix Marseille Université-CNRS, Technopôle Méditerranéen de l'Arbois, Siame, Lionel; CEREGE, UMR 7330 Aix Marseille Université-CNRS, Technopôle Méditerranéen de l'Arbois, Cordy, Jean-Marie; University of Liège, Institute for Zoology, Place Delcour 17, 4020 Demoulin, Alain; University of Liège, Department of Geography, Allée du six Août 2, 4000
Keywords:	cosmogenic nuclide dating (10Be), river terrace , Belle-Roche palaeokarst, middle Pleistocene palaeofauna, Early Palaeolithic, Ardennes massif

^{10}Be dating of the Main Terrace level in the Amblève valley (Ardennes, Belgium): New age constraint on the archaeological and palaeontological filling of the Belle-Roche palaeokarst

GILLES RIXHON, DIDIER L. BOURLÈS, RÉGIS BRAUCHER, LIONEL SIAME, JEAN-MARIE CORDY AND ALAIN DEMOULIN

Rixhon, G., Bourlès, D.L., Braucher, R., Siame, L., Cordy, J.-M. & Demoulin, A.: ^{10}Be dating of the Main Terrace level in the Amblève valley (Ardennes, Belgium): New age constraint on the archaeological and palaeontological filling of the Belle-Roche palaeokarst.

It is still disputed whether very old archaeological and palaeontological remains found in the Belle-Roche palaeocave (eastern Belgium) pertain to the Early (~1 Ma) or Middle (~0.5 Ma) Pleistocene. Here, *in situ*-produced cosmogenic ^{10}Be concentrations from a depth profile in nearby sediments of the Belle-Roche terrace (Amblève Main Terrace level) are used as an indirect solution of this chronological issue. The distribution of ^{10}Be concentrations in the upper 3 m of this profile displays the theoretically expected exponential decrease with depth. Assuming a single exposure episode, we obtain a best fit age of 222.5±31 ka for the time of terrace abandonment. However, below 3 m, the ^{10}Be concentrations show a marked progressive increase with depth. This distinctive cosmogenic signal is interpreted as the result of slow aggradation of the fluvial deposits over a lengthy interval. Modelling of the whole profile thus suggests that the onset of the terrace formation occurred at around 550 ka, with a sediment accumulation rate of ~20 mm ka^{-1}. Based on two slightly different reconstructions of the geomorphic evolution of the area and a discussion of the temporal link between the cave and Main Terrace levels, we conclude that the fossil-bearing layers in the palaeokarst pertain most probably to MIS 14–13, or possibly MIS 12–11. This age estimate for the large mammal association identified in the Belle-Roche palaeokarst and the attribution to MIS 14–13 of a similar fauna found in the lowermost fossiliferous layers of the Caune de l'Arago (Tautavel) are in mutual support. Our results therefore confirm the status of the Belle-Roche site as a reference site for the Cromerian mammal association in NW Europe.

Gilles Rixhon (grixhon@uni-koeln.de), Institute for Geography, University of Cologne, Zülpicher Straße 45, 50674 Cologne, Germany; Didier Bourlès, Régis Braucher and Lionel Siame, Aix-Marseille

Université, CNRS-IRD-Collège de France, UM 34 CEREGE, Technopôle de l'Environnement Arbois-Méditerranée, BP80, 13545 Aix-en-Provence, France; Jean-Marie Cordy, Institute for Zoology, University of Liège, Place Delcour 17, 4020 Liège, Belgium; Alain Demoulin, Department of Geography, Unit of Physical Geography and Quaternary, University of Liège, Allée du six Août 2, 4000 Liège, Belgium and FRS-FNRS, Brussels, Belgium.

The Belle-Roche archaeological and palaeontological site in eastern Belgium was discovered in the early 1980s (Cordy 1980,1982; Cordy & Ulrix-Closset 1981). Located near the northern margin of the Ardennes Massif, it represents a palaeocave in the valley of the Amblève River, one of the main intra-massif subtributaries of the River Meuse. This palaeokarst is perched ~58–60 m above the current floodplain of the Amblève and is filled with fluvial gravel overlain by a complex of slope deposits rich in macrofaunal remains and also containing Palaeolithic artefacts. These remains and their sedimentological context have been thoroughly described and analyzed (Cordy & Ulrix-Closset 1991; Cordy *et al.* 1993; Draily & Cordy 1997; Renson *et al.* 1997; Cordy 1998; Draily 1998), leading to assign the tools to an early Palaeolithic industry (Draily & Cordy 1997; Cordy 1998, Draily 1998). While this lithic industry shares many characteristics with other archaeological sites such as Kärlich and Mauer in Germany (Draily & Cordy 1997), the initially proposed age of 500±70 ka for the Belle-Roche deposits made it one of the oldest sites showing traces of human presence in continental NW Europe (Bosinski 2006).

This age was based on the presence of numerous and varied micro- and macro-mammalian remains found in association with the artefacts (Cordy *et al.* 1993). It was also supported by palaeomagnetic data revealing a normal polarity throughout the palaeokarst deposits, which Cordy *et al.* (1993) ascribed to the Brunhes chron. However, on the basis of geometric correlations between the terrace sequences of the Amblève and the lower Meuse, where more palaeomagnetic data are available (Van den Berg 1996), Renson *et al.* (1997, 1999) and Juvigné *et al.* (2005) re-interpreted the normal polarity of the Belle-Roche cave gravels, assigning it to the Jaramillo Event. Accordingly, they proposed a much older age of ~0.99 to ~1.07 Ma for the palaeokarst filling and the archaeological and palaeontological remains.

In order to resolve this major discrepancy between the palaeontological and geomorphic age estimates of the cave deposits, we focus here on the dating of the Amblève terrace, located just below the palaeokarst, which we have obtained from a Terrestrial Cosmogenic Nuclides (TCN) depth profile. The TCN dating techniques have advanced considerably during the last two decades, although their potential for geoarchaeology and palaeoanthropology has so far been largely overlooked (Akçar *et al.* 2008). The age of the Belle-Roche terrace level is indeed a key to constrain the age of the fossil-bearing layers in the cave. Not only does this terrace, called the (Younger) Main Terrace (YMT), represent a fundamental morphogenetic stage of valley evolution (Rixhon & Demoulin 2010), but its top surface is also situated only 3 m below the base of the fluvial gravels in the palaeocave. Owing to the great thickness of the terrace deposits, ten samples were collected along a depth profile for measurement of *in situ*-produced ^{10}Be concentrations. Beside the ^{10}Be age estimate for the terrace, involving complex modelling of the data, we discuss the geomorphic evolution of the area between the times of cave filling and terrace formation, in order to define the temporal relationship between the two events and derive a new age for the Belle-Roche archaeological and palaeontological remains.

Site location and description

Located in the northern part of the Ardennes, in eastern Belgium (Fig. 1A), the Belle-Roche site lies in the lower Amblève valley, approximately 20 km south of Liège (Fig. 1B). During incision into the uplifted Palaeozoic Ardennes massif, the Amblève River has developed a large entrenched meander at Belle-Roche, about 2 km upstream of the confluence between the Amblève and Ourthe rivers (Fig. 1C). The palaeokarst and the studied remnant of the Main Terrace (hereafter named Belle-Roche terrace) are both situated on the right-hand, inner valley side of the meander, at respective elevations of ~158 m a.s.l. (top of the alluvial sediments within the palaeocave, see below) and ~154 m a.s.l. (terrace upper surface). The elevation of the modern floodplain of the Amblève is ~101 m a.s.l. in the meander, implying >110–120 m Pliocene–Quaternary incision through Carboniferous limestones in this lower reach (Fig. 1D), about half of which has occurred since the formation of the Main Terrace. Belle-Roche cave and terrace have been cut into the northern, subvertical limb of the limestone syncline that rests on Devonian sandstones forming the adjacent anticlinal ridges to the N and the S (Fig. 1D).

The Belle-Roche palaeokarst: archaeological and palaeontological remains

General description and filling deposits

The Amblève formed the Belle-Roche karstic level when its valley-floor was approximately 56–58 m above its present floodplain. The palaeocave belongs to a karstic network whose general orientation follows the bedding of the limestones (Fig. 2A). Four horizontal galleries, roughly parallel to each other, have been discovered thus far (Fig. 2A). Karstic shafts developed through differential dissolution of dolomitized levels are associated with these galleries. The cumulated width of the three interconnected galleries (II, III & IV) in which palaeontological remains and artefacts were found is approximately 25 m (Fig. 2A).

At the base of the cave filling, up to 1 m-thick alluvial sediments consisting of cm-sized, well sorted gravels embedded in a sandy–silty matrix lie on limestone bedrock at an elevation of 157 m a.s.l. (Juvigné *et al.* 2005) (Fig. 2B). Their petrographical composition (mainly quartz and quartzite pebbles derived from the Stavelot massif to the east) and the orientation of the gravels indicate that these sediments were deposited by the Amblève and form an “intrakarstic” alluvial terrace of the river (Cordy *et al.* 1993; Juvigné *et al.* 2005; Rixhon & Demoulin 2010). These river deposits are devoid of archaeological or palaeontological remains. They are overlain by three superposed layers of slope deposits, brought into the cave by runoff or solifluction (Fig. 2B). Up to 2.5 m thick and capped by a calcite flowstone, these deposits completely fill the cave, reaching the cave roof at an elevation of ~160 m a.s.l. (Juvigné *et al.* 2005). They mainly consist of clayey silts containing numerous angular, up to boulder-sized, limestone clasts, with some reworked gravel at their base (Fig. 2B, C), and show upward enrichment in reddish decalcification clay and limestone clasts (Fig. 2B). The deposits are poorly sorted and the clasts do not show any well-defined orientation (Cordy *et al.* 1993). Three sub-units are distinguished, based on their nature and named “lower silt”, “middle rubble” and “upper rubble” from bottom to top (Cordy *et al.* 1993; Renson *et al.* 1997, 1999; Juvigné *et al.* 2005). All the sub-units contain faunal and archaeological remains (see below).

Fauna remains

The palaeontological remains of the Belle-Roche palaeokarst are extremely rich, not only in terms of quantity but also diversity. Several tens of thousand of bone and teeth fragments from at least 50 different species of macro- and micromammals have been found, including carnivores, insectivores, chiropters, artiodactyls, perissodactyls, lagomorphs, and rodents (Cordy *et al.* 1993). Faunal fossils are present throughout the slope deposits (*i.e.,* in the upper three sub-units) in reworked position, as bone fragments are rarely found in anatomic connection (Cordy *et al.* 1993). Macrofaunal remains notably include the following species (Cordy *et al.* 1993): *Canis mosbachensis* (Fig. 3A)*, Hemitragus bonali* (Fig. 3B)*, Panthera onca gombaszoegensis* (Fig. 3C)*, Panthera leo fossilis* (Fig. 3D)*, Ursus deningeri* (Fig. 3E). Carnivores are particularly well represented and diverse among macro-mammal remains, with *Ursus deningeri* by far the most abundant species (Cordy *et al.* 1993). Microfaunal remains are mainly from rodents, amongst which *Arvicola cantiana* (Fig. 3F) is important.

In terms of palaeoecology, the cave was probably used as a hibernation and/or parturition place by *Ursus deningeri*, whereas it presumably acted as a shelter or as a lair for other carnivores (Cordy *et al.* 1993). As these predators came into the cave, prey remains were also probably dragged inside, which explains the presence of herbivore fossils.

Lithic artefacts

Lithic tools are found only in the uppermost infill layer of the Belle-Roche cave (“upper rubble”, Cordy *et al.* 1993, Renson *et al.* 1997). They were probably transported by solifluction into the palaeokarst, whereas former humans lived in the immediate vicinity of the cave entrance (Draily & Cordy 1997).

Flint represents the main material used in the Belle-Roche industry (Fig. 4; Cordy *et al.* 1993; Draily & Cordy 1997). Altogether, about 110 artefacts have been identified (Draily & Cordy 1997). Most are struck or splitting products (~86 %) of small dimension (maximum 7 cm in length), the rest corresponding to shaped tools. The struck pieces are primarily flint flakes (71), some having been retouched as scrapers (Fig. 4A), with subordinate cores (24). Chopping-tools (Fig. 4B), choppers and, in smaller numbers, bifaces (Fig. 4C) have been recognized amongst the shaped tools. Finally, short, deep angular notches may be observed on two bones of *Ursus deningeri* (Fig. 4D); they correspond presumably to ‘cut-marks’ made during anthropogenic skin or flesh removal (Cordy *et al.* 1993).

Two main features characterize the artefacts (Draily & Cordy 1997), namely their abrasion (slightly rounded edges), making the identification of some tools difficult (Cordy *et al.* 1993), and the lack of sophistication, which points to an old and primitive lithic industry inherited from the early Palaeolithic (Cordy *et al.* 1993; Draily & Cordy 1997).

Existing chronological framework

In this section, we review the chronological data available so far for the palaeokarst and the Belle-Roche terrace and discuss their relative significance.

Palaeontology

The variety of the macromammal remains present in the slope deposit layers of the Belle-Roche cave allows a first estimate of their age. In particular, the association of *Canis mosbachensis, Dicerorhinus etruscus, Equus mosbachensis, Hemitragus bonali, Panthera onca gombaszoegensis, Panthera leo fossilis, Ursus deningeri, Xenocyon lycaonoides*, and rodents such as *Arvicola cantiana* and *Pitymis gregaloides* is characteristic of the late Cromerian (Cordy *et al.* 1993). According to theses authors, this palaeofauna association is probably coeval with those found at the sites of Mauer and Mosbach in Germany and in the caves of Escale in France and Atapuerca in Spain. It defines a biozone that has been associated with MIS 15 or 13 (Cordy 1982, 1992). Therefore, the fossil-bearing layers of Belle-Roche and, consequently, the associated lithic industry were dated to 500±70 ka (Cordy *et al.* 1993).

Moreover, the upward evolution of the palaeontological association, and especially of the microfaunal composition, allowed Cordy *et al.* (1993) to draw palaeoclimatic inferences, namely identifying a transition from cold to temperate conditions. Indeed, the typically boreal rodents (*Dicrostonyx* sp.*, Lagurus* sp.*, Lemmus* cf. *Lemmus*, *Ochotona* cf. *Pusilla*) and, among the macromammals, the reindeer (*Rangifer tarandus*) observed in the lower part of the slope deposits are progressively replaced by rodents like *Apodemus* sp. and temperate forest species such as *Capreolus capreolus* cf. *sussenbornensis* and *Cervus elaphus* cf. *acoronatus* in the upper layer, where the artefacts have been found. This climatic transition, which features a temperature gradient (from periglacial to temperate conditions) and a humidity gradient (from dry to wet), was confirmed by the analysis of clay minerals (Cordy *et al.* 1993).

Radiometric dating

Another age indication was derived from U/Th dating of the calcite flowstone that seals the fossiliferous layers of the cave (Fig. 2C). This provided an age of >350 ka (Gascoyne & Schwarcz 1985; Gewelt 1985). This minimum age for the speleothem does not contradict the palaeontological age estimate of the underlying layers.

Palaeomagnetism

Palaeomagnetic measurements were carried out in the fine fraction of the cave filling (Fig. 2C; Cordy *et al.* 1993) and in silty layers interspersed in the Belle-Roche terrace gravels (Juvigné *et al.* 2005). All of these revealed a normal polarity (Fig. 2C), except one situated at the base of the terrace deposits, which displayed a questionable intermediate polarity (Juvigné *et al.* 2005).

These palaeomagnetic data led to different interpretations. Based on the temporal indication derived from the palaeofauna, Cordy *et al.* (1993) assigned the normal polarity of the cave deposits to the Brunhes chron. However, Renson *et al.* (1997, 1999) and Juvigné *et al.* (2005) disputed this interpretation on the basis of geometric terrace correlations between the Amblève, Ourthe, and Meuse valleys and palaeomagnetic data from the lower Meuse in the Maastricht area (Van den Berg 1996). There, the Main Terrace complex of the Meuse, comprising three closely spaced alluvial levels, represents a major geomorphic marker that also marks the sharp transition, in the transverse profile of the main Ardennian valleys, between a broad Early Pleistocene valley with wide terrace surfaces and a nested narrow Middle Pleistocene valley characterized by steeper slopes and more confined and scarcer terraces (*e.g.* Meyer & Stets 1998; Van Balen *et al.* 2000; Rixhon & Demoulin 2010, Rixhon *et al.* 2011). According to Van den Berg (1996), the higher levels of the Main Terrace complex (terraces of Sint Pietersberg 1 and 2) in the lower Meuse were formed at the end of the Matuyama period while its lower level (Sint Pietersberg 3) is coeval with the Matuyama/Brunhes boundary (~0.78 Ma). In his view, the normal polarity found in the Sint Geertruid terrace, overlying the Main Terrace complex, is then inherited from the Jaramillo Event (~0.99 to ~1.07 Ma). Based on geometric correlations between terraces in the lower Meuse (Juvigné & Renard 1992), the lower Ourthe (Cornet 1995), and the Amblève, Renson *et al.* (1997, 1999) concluded that the Belle-Roche terrace and the cave gravels were the Amblève equivalents of, respectively, the Sint Pietersberg and Sint Geertruid terraces. Consequently, they attributed the normal polarity of the cave filling to the Jaramillo Event, which led them to give an age of ~1 Ma to the archaeological and palaeontological remains. Relying on new palaeomagnetic data in the Belle-Roche terrace, Juvigné *et al.* (2005) finally added that this terrace had been abandoned near the Matuyama/Brunhes boundary. It should, however, be noted that this conclusion is consistent with the palaeomagnetic interpretation of Van den Berg (1996) in the lower Meuse, but not with that of van Balen *et al.* (2000), who assign all levels of the Main terrace complex at Maastricht to the Brunhes chron and correlate the Belle-Roche cave gravels with the higher level of this complex. In summary, the palaeomagnetic data at Belle-Roche and in the Maastricht area tend to obscure the picture rather than helping to constrain the age of the cave deposits.

Sampling site: the Belle-Roche Terrace

The terrace, located a few meters downslope of the palaeokarst, is ~425 m long and ~225 m wide (Fig. 1B). While the elevation of the current floodplain is about 101-102 m, the mean height of the terrace surface is about 153-154 m, corresponding to a mean relative elevation of ~52 m (Fig. 1D). The Belle-Roche terrace has been assigned to the youngest Main Terrace level of the lower Amblève (Rixhon & Demoulin 2010; Rixhon *et al.* 2011). Main reasons for this are (i) the elevation of the terrace surface relative to the modern floodplain, similar to the Main Terrace elevation in the lower Ourthe valley (Cornet, 1995), (ii) the large extent of the fluvial remnant, and (iii) the unusually great thickness of alluvial sediments (Juvigné *et al.* 2005; Rixhon *et al.* 2011).

The altitude of the terrace base is not known exactly. Indeed, up to 6.25 m-deep trenches (Juvigné *et al.* 2005; Rixhon *et al.* 2011) did not reach the bedrock in the central part of the terrace (Fig. 5A, B), and the estimated elevation of 145 m a.s.l. for the bedrock/gravel contact relies on seismic sounding data (Juvigné *et al.* 2005) (Fig. 5A). This implies a sediment thickness of ~8 m in the central part of the terrace (Fig. 5A). This unusual thickness (at least in valleys in the Ardennes) does not appear to be related to karstic collapse. According to Juvigné *et al.* (2005) and to our field observations, the fluvial gravel of the Belle-Roche terrace is preserved in its original position.

The top surface of the Belle-Roche terrace displays a clear transverse slope towards the valley axis at the trenching site (Fig. 5A). This may be explained partly by its marginal burial under slope deposits (Fig. 5A), and partly by recent erosion of the terrace deposits, as witnessed by the development of a gully currently cutting into the middle of the terrace (Fig. 1C). We dug the trench at 153 m a.s.l. in a place of the eastern forested part of the terrace where field observations indicate that erosion was limited and colluviation absent (see below).

Overlain only by the ~20-cm-thick modern soil, the fluvial sediments exposed in the ~6.25 m-deep main trench T1 are coarse gravels and cobbles, mainly quartz and quartzites originating from the Stavelot massif to the east, embedded in a fine-grained matrix (Fig. 5B). They display no visible stratification. A few ice-rafted boulders (Ardennes quartzites) are also present, similar to those observed in the Meuse deposits north of Liège (De Moor & Pissart 1992). This facies is typical of terrace deposits in the Ardennes (Rixhon *et al.* 2011).

In one of the four trenches excavated in the Belle-Roche terrace by Juvigné *et al.* (2005) very close to our trench T1, the presence of several silt and sand lenses interspersed within the gravels were reported (Juvigné *et al.* 2005). These authors interpreted these features as indicating sedimentation in a braided-river environment. Moreover, syngenetic cryoturbation of the sediments at depths greater than 2 m confirmed aggradation under cold conditions, probably in several episodes.

We excavated a second trench (T2, Fig. 5A) in the very upper part of the landform. There, the fluvial terrace sediments were buried underneath ~1.1 m of colluvium. The latter clearly exhibited a slope deposit facies: matrix-supported, including numerous angular limestone clasts of local origin and scarce subrounded pebbles, probably reworked from a higher-level terrace (Fig. 1D). Similar in facies to the slope deposits in the cave, this colluvial wedge points to solifluction. In this marginal location in the close vicinity of the hillslope, the bedrock was reached at a depth of ~3.6 m, below ~2.5-m-thick terrace gravels (Fig. 5A).

We sampled trench T1. Although the sloping surface of the terrace might at first glance raise fears of a slope deposit component or of remobilization by slope processes, all observations demonstrate that these are river terrace deposits in their original position in T1: (i) the altitude of the trench (153 m a.s.l.) is similar to that of the surface of the large horizontal western part of the terrace (which is cultivated and where unfortunately we were not allowed to excavate), (ii) there are no local angular clasts, only rounded elements, (iii) fluvial sedimentary structures are present (Juvigné *et al.* 2005), (iv) where observed (e.g., in T2), slope deposits show a completely different facies, (v) the quartz content in T1 gravels (<20%) is typical of the main and lower terraces, as opposed to much higher percentages in higher terrace material (>30 to >50%) (Juvigné *et al.* 2005).

Ten samples were collected for ^{10}Be concentration measurements at regular depth intervals along a vertical profile of approximately 6.25 m depth (Fig. 5B). The shallowest sample was taken at ~0.6 m and the deepest at ~6 m below the surface, a depth at which the limestone bedrock was still not reached (Fig. 5B). Each sample consisted of a single quartz or quartzite pebble or cobble.

Sample preparation and ^{10}Be concentration measurements

The chemical treatment and the AMS measurement of the samples were performed at the French Cosmogenic Nuclides National Laboratory (LN2C; CEREGE, Aix-en-Provence). The chemical procedures relative to the preparation of ^{10}Be concentration measurements were adapted from Brown *et al.* (1991) and Merchel & Herpers (1999). All the Belle-Roche terrace data reported in this study (Table1) have been obtained at ASTER (Accélérateur pour les Sciences de la Terre, Environnement et Risques, Aix-en-Provence), the French AMS national facility (Arnold *et al.* 2010). Table 1, showing the ^{10}Be concentration measurements from our quartz samples, also reports mandatory parameters in cosmogenic nuclide dating such as the latitude and the altitude of the terrace location, hence the scaling factor (see below), and the sample depth expressed both in cm and g cm^{-2}, the latter unit normalizing to the material density. After sieving (to obtain the 0.25–1.0 mm fraction), sediment samples passed through magnetic separation, and the non-magnetic fraction underwent selective etchings in fluorosilicic and hydrochloric acids to eliminate all mineral phases but quartz. Quartz minerals then underwent a series of selective etching in hydrofluoric acid to eliminate potential surface contamination by ^{10}Be produced in the atmosphere. The cleaned quartz minerals were then completely dissolved in hydrofluoric acid after the addition to each sample of ~100 µl of an in-house carrier solution ((3.025±0.009)x10^{-3} g ^{9}Be g^{-1} solution) prepared from a deep-mined phenakite (Merchel *et al*. 2008). Hydrofluoric and Perchloric fuming was used to remove fluorides and both cation- and anion-exchange chromatography were used to eliminate iron, aluminium, manganese and other elements. Beryllium oxide was mixed into 325 mesh niobium powder prior to measurements by Accelerator Mass Spectrometry (AMS). Beryllium-10 data were calibrated directly versus the National Institute of Standards and Technology standard reference material NIST SRM 4325 using an assigned $^{10}Be/^{9}Be$ value of (2.79±0.03)x10^{-11} (Nishiizumi *et al.* 2007) and a ^{10}Be half-life of (1.387±0.012)x10^{6} years (Korschinek *et al*. 2010; Chmeleff *et al.* 2010).

Analytical uncertainties (reported as 1σ) include those associated with AMS counting statistics, AMS external error (0.5%) and chemical blank measurement. Long-term AMS measurements of a chemically processed blank yield ratios in the order of (3.0±1.5) x10^{-15} for $^{10}Be/^{9}Be$. Cosmocalc add-in for excel (Vermeesch 2007) has been used to calculate sample-thickness scaling (with an attenuation coefficient of 160 g cm^{-2}) and atmospheric pressures. The ^{10}Be production rate was scaled following Stone (2000) with a sea-level high latitude production rate of 4.5±0.3 at g^{-1} a^{-1}. There was no topographic shielding to deal with at our sampling place (shielding factor of 1).

Three main types of secondary particles related to the cosmic-ray shower are involved in the *in situ*-production of cosmogenic ^{10}Be in quartz: fast nucleons (essentially neutrons), stopping (or negative) muons and fast muons (Gosse & Phillips 2001). Each of these particles has its own effective attenuation length; here, we used the values of 160 g/cm^2 for fast neutrons (Lal 1991), and 1500 g/cm^2 and 4320 g/cm^2 for stopping and fast muons, respectively (Braucher *et al.* 2011). Muon contributions in this study are based on Braucher *et al.* (2011) as well. Using both the measured and theoretical concentrations at various depths (integrating both the nucleaon and muon contributions), inversion of the ^{10}Be concentrations with depth-profile may be utilized to determine the denudation and exposure age affecting the deposit since its abandonment (*e.g.* Siame *et al*. 2004; Braucher *et al.* 2009). However, the Belle-Roche concentration profile satisfies the basic condition of this approach (i.e., that an exponential curve may be fitted to the data) only in its upper half, where the five samples collected between ~0.6 m and ~3 m depth indeed show an exponential decrease of ^{10}Be concentrations with increasing depth (Fig. 6A). Below 3 m, the remaining samples clearly record a progressive enrichment in ^{10}Be with depth (Fig. 6A).

We decided therefore to model separately these two disconnected parts of the profile. Determination of the exposure time of the terrace gravel was performed using the five upper samples (Fig. 6B). In contrast, the unusual cosmogenic signal recorded in the lower part of the profile compelled us to build up a specific model that had to match the ^{10}Be concentrations at depths ≥3 m and to integrate the previously calculated exposure time (Fig. 6C). Both procedures and their respective results are presented below.

Model procedures and age determination

Upper part of the profile (0 – 3 m depth)

The χ^2 - Monte Carlo modelling approach developed by Braucher *et al.* (2009) was applied to the five upper ^{10}Be data of the profile (Fig. 6B) in order to estimate the four basic parameters entailed in cosmogenic nuclide dating of terrace deposits (Rixhon *et al.* 2011). These parameters are (i) the terrace exposure time (t_{exp}), (ii) the denudation rate (ε), (iii) the ^{10}Be inheritance, and (iv) the density of the alluvial material (ρ). As Braucher *et al.* (2009) stated that the model procedure is very sensitive to density when one wants to determine both the exposure time and the denudation rate from a ^{10}Be concentration depth profile, we treated density as a free parameter similar to t_{exp}, ε and inheritance.

This was all the more necessary as it is very difficult to measure a density value in the field accurately, especially in heterogeneous terrace deposits. Thus, density was free to adjust within a plausible range of values (1.8 to 2.4 g cm^{-3}), assuming that it remains constant throughout the profile.

The four-parameter adjustment of the upper Belle-Roche profile yielded an exposure time of 222.5±31 ka, corresponding to the abandonment time of the terrace (Rixhon *et al.* 2011). In addition to a small inherited content in ^{10}Be (20.10^3 at g^{-1}) and a density estimate of 2.3 g cm^{-3}, the model best fit yielded a denudation rate of ~4.5 m Ma^{-1} since abandonment of the terrace (Rixhon *et al.* 2011). This implies a limited lowering (~1 m) of the terrace surface at the trench location, which is consistent with field observation. As the concentration steady-state (dynamic equilibrium between ^{10}Be production on one hand, ^{10}Be disintegration and erosion on the other hand) has not yet been reached, the exposure time is fairly well constrained. However, owing to the non-zero denudation rate, the associated uncertainty is relatively high (~15%).

Lower part of the profile (3 – 6 m depth)

The anomalous ^{10}Be enrichment at depth requires a specific conceptual approach and an adapted treatment of the lower half of the sampling profile. Rixhon *et al.* (2011) suggested that this high ^{10}Be content was acquired during a long-lasting phase of progressive, slow accumulation of river sediments. This interpretation is in line with the conclusions of other studies that treated profiles highlighting similar ^{10}Be enrichment at depth (Brown *et al.* 1994; Nichols *et al.* 2002, 2005). The remarkable fit of the lower half of the Belle-Roche profile, based on four ^{10}Be concentration values (Fig. 6C), is therefore very unlikely to result from inheritance, a highly stochastic process by nature. At most, inheritance variability, as suggested by Hidy *et al.* (2010) to explain erratic ^{10}Be enrichment at depth, allows the presence of one outlier (sample Be07-BR21), in the lower part of the profile (Fig. 6C).

In terms of processes, the only way to fit the concentration data from the lower half of the profile satisfactorily is indeed to assume progressive burial of this part of the profile, followed by rapid (geologically instantaneous) accumulation of the four upper meters (featuring the classical exponential ^{10}Be decrease with depth), and then continuous exposure of the whole deposit. Two geomorphic processes might have combined to produce such a scheme, implying slow overall aggradation and transient rapid accumulation, namely the spatial instability of braided channels and/or temporal alternation of sedimentation and erosion within a climate-driven cut-and-fill system. These processes resulted in regular renewal of the upper part of the alluvial cover, and hampered *in situ* ^{10}Be preservation therein, while the deeper immobilized part of the cover, though less exposed to the cosmic rays, was able to store the produced ^{10}Be. The 4-m thickness of the upper fast-accumulation layer is consistent with the gravel thicknesses observed in the modern Amblève floodplain. When the deposit aggraded, its deep ^{10}Be-accumulating part was also progressively thickened. At the final stage, just before the Amblève started to incise into its YMT floodplain, the lower part of the gravels had accumulated ^{10}Be in proportion to their residence time in the deposit (i.e., in proportion to depth), whereas the upper part had rapidly built up during the preceding glacial and was almost devoid of *in situ*-produced ^{10}Be. When incision began, this upper layer was in turn immobilized in the terrace and started to accumulate ^{10}Be following the usual exponential depth profile.

While Rixhon *et al.* (2011), following the above reasoning, obtained a long-term aggradation rate of ~25 mm ka^{-1} for the slow accumulation component, improved values for fast and stopping muon contribution recently published by Braucher *et al.* (2011) lead to a slightly slower rate of 20 mm ka^{-1}. Based on this rate, progressive burial of the deepest sample (Be07-BR20) required about 225 ka. However, according to the results of seismic soundings (Juvigné *et al*. 2005), we know that the base of the terrace gravels most likely lies 2-2.5 m below this sample, which suggests that the total burial time should have been of at least 325 ka. Modelling of the complete profile history (slow burial – final stage of rapid accumulation – exposure) fits the data remarkably well, with the exception of one outlier (Fig. 6C), and yields a minimum age of ~550 ka for the time when the Amblève started to accumulate gravels at the YMT level.

Discussion

Geomorphological evolution at Belle-Roche and the age of the cave deposits

Although several error sources (assumption of constant accumulation rate, uncertainty about actual gravel thickness, modelling error on exposure time) make the uncertainty on the minimum age of the YMT deposits at Belle-Roche far from negligible, the greatest difficulty in deriving an age estimate of the fossiliferous and artefact-bearing deposits in the cave results from the indirect way in which the link between the cave filling and the subaerial terrace is established. This link depends on several assumptions that are made on the geomorphic evolution of the site and leads to two contrasting possible reconstructions, both of which leave some issues unanswered but agree in locating the archaeological and palaeontological remains in the middle part of the Middle Pleistocene.

With the exception of van Balen *et al*. (2000), it has so far always been admitted that deposition of the cave gravels was contemporaneous with subaerial floodplain development at the same elevation, that is, prior to the formation of the lower-lying Belle-Roche terrace (Cordy *et al.* 1993; Renson *et al.* 1997, 1999; Juvigné *et al.* 2005). Consequently, as there is no other terrace level intercalated between the cave and the terrace, and following the widely accepted correlation between terrace levels and glacial cycles (e.g. Antoine 1994; Vandenberghe 1995; Bridgland & Westaway 2008), the cave gravels were supposed to have been deposited during the glacial just before the one when the Belle-Roche terrace formed. Furthermore, the slope deposits in the cave, which encompass one full glacial cycle from cold to temperate conditions, accumulated only after flowing water had abandoned the karstic conduit, most likely because of valley incision. As Renson *et al.* (1997, 1999) already noted, there was probably no significant hiatus between deposition of the gravels and the overlying slope deposits, which suggests that the latter reached the cave in the next glacial, i.e., that during which the Belle-Roche terrace started to form (~550 ka). In this reconstruction, the palaeontological remains belong therefore to the glacial/interglacial cycle MIS 14/MIS 13 and the artefact-bearing layer in particular to MIS 13 (Fig. 7).

However, the above interpretation raises two issues. Firstly, as the cave gravels are situated ~12 m above the base of the Belle-Roche terrace, it implies a rather surprising river incision history in which a rapid 12-m-deep incision would have been followed by a ~325-ka-long phase of stability (aggradation of the Belle-Roche terrace), and then renewed rapid incision at ~223 ka. Secondly, in the lower Amblève, remnants of the terrace level just above the Belle-Roche terrace are observed some ~14 m higher than the YMT (Rixhon & Demoulin 2010), thus also 10 m higher than the cave gravels. If flow occurred in the cave in relation with this higher terrace, the passage should display the circular or elliptic section typically observed for tubes in the phreatic zone (e.g. Audra & Palmer 2013), which is not the case.

The shape of the conduit and the grain size of its fluvial deposits (i.e. a bed-load material much smaller than the bed-load of the subaerial channel) rather suggest that the cave only carried overflow during high-flow episodes (e.g., spring snowmelt during a cold stage) and, consequently, that it was located somewhat higher than the contemporaneous floodplain. According to this interpretation, the cave gravels would therefore be coeval to the Belle-Roche terrace itself. This apparently strongly loosens the constraint on the age of the gravel, as aggradation of the Belle-Roche floodplain extended over three glacial cycles. However, the >350 ka dating by U/Th of the flowstone capping the fossiliferous deposits sets a minimum age for the cave filling and namely involves that the upper artefact-bearing layer pertains to MIS 11 at the latest (Fig. 7). This would imply a MIS 12 age for the lower slope deposits and allow gravel accumulation in the conduit mainly during MIS 14 (Fig. 7). Taking into account the slow aggradation occurring in the palaeo-floodplain, this interpretation suggests that the conduit was accessible, and needed to evacuate overflow, when the Belle-Roche valley bottom was still narrow. The conduit became inactive once the floodplain had widened and flooding no longer reached the level of the palaeocave. In comparison with the first geomorphic interpretation, the only weakness of this alternative reconstruction might lie in the relative height of an active conduit, for which they are few precedents in the literature (Anthony & Granger 2004). On the other hand, significant flood heights during snowmelt in the narrow Ardennian valleys related to strong periglacial conditions (Pissart 1995; Rixhon & Juvigné 2010) may give an answer to this issue. We note also that the latter interpretation does not exclude that the conduit was already inactive by MIS 14, thus better supporting the observed continuity from gravel to slope deposit accumulation. In this case, the lowermost infill layers containing the cold-climate fossils would belong to the MIS 14, and the uppermost layer with temperate-climate fossils and artefacts to the MIS 13 (Fig. 7).

In summary, both reconstructions yield an age between 500 and 400 ka (MIS 13 or 11) for the artefact-bearing upper layer of the cave filling and, in any case, place the whole sequence, from the cave gravels to the Belle-Roche terrace deposits, at ~675 ka at the earliest (MIS17–16 transition, Lisiecki & Raymo 2005) (Fig. 7). This places all palaeomagnetic data obtained at Belle-Roche within the Brunhes chron (Fig. 7), definitely invalidating the correlation of normal polarity in the cave gravels with the Jaramillo Event proposed by Renson *et al.* (1997, 1999) and Juvigné *et al.* (2005). Despite the slight age discrepancy between our two schemes for the geomorphic evolution at Belle-Roche, they agree in confirming the Cromerian age of the palaeofauna in the Belle-Roche cave and unequivocally discarding the concurrent age estimate of ~1 Ma claimed by Renson *et al.* (1997, 1999) and Juvigné *et al.* (2005).

Implications of the Belle-Roche ^{10}Be age for biostratigraphic correlations and early Palaeolithic industries in NW Europe

The ~1 Ma age of the archaeological and palaeontological remains in the Belle-Roche palaeokarst (Renson *et al.* 1997, 1999; Juvigné *et al.* 2005) questioned the use of palaeofauna associations as a robust chronological marker for the Quaternary, at least regarding this site. Our independent ^{10}Be dating of the neighbouring Belle-Roche terrace reinstitutes palaeontological associations as a reliable chronological marker for the Belle-Roche palaeocave.

As shown by Figure 7, several studies recently dealt with biostratigraphic reconstructions based on carnivorous (Croitor & Brugal 2010), herbivorous, and rodent species (Eisenmann 1991; Chaline *et al.*1993; Cerdeño 1998; Van der Made 2001; Mancini *et al.* 2012) in northern Europe. Regarding carnivores, most species present in the Belle-Roche palaeokarst are recorded over a lengthy Quaternary time span and are therefore not biostratigraphically discriminatory (Fig. 7). However, the unique discovery of a complete skull of *Panthera onca gombaszoegensis* (Fig. 3C) in the cave filling turned the Belle-Roche palaeokarst into a reference site for this feline. Rodents also provide limited age information, even if *Arvicola cantiana* (Fig. 3E) is a useful marker within the Middle Pleistocene microfauna. In contrast, the stratigraphic range of some herbivores recognized in the cave is shorter and therefore more discriminatory (Fig. 7, e.g. *Bison schoetensacki* and *Cervus elaphus acoronatus*).

Many of the large mammals species identified in the Belle-Roche palaeokarst were also found in the Caune de l'Arago site, Tautavel (Moigne *et al.* 2006). The two lowermost fossiliferous levels of the latter cave (units 1 and 2 from the middle complex) revealed the following species: *Bison schoetensacki, Canis mosbachensis* (Fig. 3A), *Cervus elaphus, Equus mosbachensis, Felix silvestris, Hemitragus bonali* (Fig. 3B), *Rangifer tarandus, Ursus deningeri* (Fig. 3E) and *Vulpes praeglacialis*. The striking similarity in faunal association between both sites argues for contemporaneity, further reinforced by the like attribution of the Caune de l'Arago fossil-bearing units 1 and 2 to MIS 14 and 13, respectively (Moigne *et al.* 2006). With its more than 50 indexed species, the Belle-Roche palaeokarst therefore represents a prime reference site for the late Cromerian palaeofauna in NW Europe.

Although the potential of TCN dating methods in archaeological issues has generally been overlooked (Akçar *et al.* 2008), two different approaches have been explored. Firstly, ^{10}Be concentrations may be directly measured in siliceous artefacts (Ivy-Ochs *et al.* 2001; Verri *et al.* 2004, 2005). However, this technique is more effective in identifying flint supply strategies than in producing reliable surface exposure dating of the artefacts (Verri *et al.* 2004, 2005). Secondly, archaeological layers in caves may be dated by the $^{26}Al/^{10}Be$ burial technique (Granger & Muzikar 2001). Although this method has proved effective in dating lower Pliocene hominid remains (Partridge *et al.* 2003), it suffers from recurrent large age uncertainties (often >0.1 Ma), chiefly due to analytical errors in ^{26}Al AMS measurements. Therefore, even though burial dating of the Belle-Roche cave gravels would theoretically be possible, the age estimate would be affected by such a large error, particularly as they lie only 3.5 m below the topographic surface, which introduces an additional bias due to post-burial production (Granger & Muzikar 2001). Finally, while we conclude here that the Belle-Roche lithic industry pertains to MIS 13 or 11, we must acknowledge that the site has lost much of its archaeological uniqueness since recent studies have involved the discovery and dating of artefacts as old as early Middle Pleistocene, and even late Early Pleistocene in other archaeological sites of NW Europe (e.g. Parfitt *et al.* 2005, 2010; Bridgland *et al.* 2006).

Conclusion

Complex modelling of the ^{10}Be concentration profile obtained from the Belle-Roche terrace in the lower Amblève valley has allowed separate estimates of the aggradation and subsequent exposure times of the terrace gravels, yielding ages of ~550 and ~223 ka for the establishment of the terrace level and its abandonment, respectively. Two geomorphic scenarios, between which we cannot so far decide, were then envisaged to derive the age of the fossil-bearing deposits in the Belle-Roche cave from the ^{10}Be age of the terrace. Assuming that the fluvial gravels in the cave formed either prior to or contemporaneously with the Belle-Roche terrace, our interpretations require the fossil-bearing deposits to be assigned respectively to MIS 14–13 or to MIS 14–13 and 12–11. Despite this possible discrepancy, our both geomorphic reconstructions thus confirm the original estimate of (500±70) ka (MIS 14–13) inferred from the palaeofaunal association (Cordy *et al.* 1993). In any case, they also invalidate the more recent ~1 Ma estimate of Renson *et al.* (1997, 1999) and Juvigné *et al.* (2005). Our results also confirm the status of the Belle-Roche site as a reference site for the Cromerian mammal association in NW Europe.

Acknowledgments. – We express our warmest thanks to Jef Vandenberghe, Pierre Antoine and an anonymous reviewer for their thoughtful and constructive comments on an earlier version of this article. David Bridgland is acknowledged for having improved the English of the manuscript. We are also indebted to Camille Ek for fruitful discussion about the proposed geomorphic scenarios. M. Arnold, G. Aumaître, and K. Keddadouche are warmly thanked for their invaluable assistance during ^{10}Be measurements at the ASTER AMS national facility (CEREGE, Aix-en-Provence), which is supported by the INSU/CNRS, the French Ministry of Research and Higher Education, the IRD and the CEA.

References

Akçar, N., Ivy-Ochs, S. & Schlüchter, C. 2008: Application of in-situ produced terrestrial cosmogenic nuclides to archaeology: A schematic review. *Eiszeitalter und Gegenwart 57*, 226–238.

Anthony, D. & Granger, D. 2004: A late Tertiary origin for multilevel caves along the western escarpment of the Cumberland Plateau, Tennessee and Kentucky, established by cosmogenic ^{26}Al and ^{10}Be. *Journal of Cave and Karst Studies 66*, 46-55.

Antoine, P. 1994: The Somme valley terrace system (northern France); a model of river response to Quaternary climatic variations since 800.000 BP. *Terra Nova 6*, 453-464.

Arnold, M., Merchel, S., Bourlès, D., Braucher, R., Benedetti, L., Finkel, R., Aumaître, G., Gottdang, A. & Klein, M. 2010: The French accelerator mass spectrometry facility ASTER: improved performance and developments. *Nuclear Instruments and Methods in Physics Research Section B: Beam Interactions with Materials and Atoms 268*, 1954–1959.

Audra, P. & Palmer, A. N. 2013: The vertical dimension of karst: controls of vertical cave pattern. *In* Shröder, J. & Frumkin, A. (eds.): *Treatise on Geomorphology 6*, *Karst Geomorphology*, 186–206. Academic Press, San Diego.

Bosinski, G. 2006: Les premiers peuplements de l'Europe centrale et de l'Est. *Comptes Rendus - Palevol 5*, 311–317.

Braucher, R., Del Castillo, P., Siame, L., Hidy, A. J. & Bourlès, D. L. 2009: Determination of both exposure time and denudation rate from an *in situ*-produced ^{10}Be depth profile: A mathematical proof of uniqueness. Model sensitivity and applications to natural cases. *Quaternary Geochronology 4*, 56–67.

Braucher, R., Merchel, S., Borgomano, J. & Bourlès, D. L. 2011: Production of cosmogenic radionuclides at great depth: A multi element approach. *Earth and Planetary Sciences Letters 309*, 1–9.

Bridgland, D. R. & Westaway, R. 2008: Climatically controlled river terrace staircases: A worldwide Quaternary phenomenon. *Geomorphology 98*, 285–315.

Bridgland, D., Antoine, P., Limondin-Lozouet, N., Santisteban, J., Westaway, R. & White, M. 2006: The Palaeolithic occupation of Europe as revealed by evidence from the rivers: data from IGCP 449. *Journal of Quaternary Science 21*, 437-455.

Brown, E., Edmond, J., Raisbeck, G., Yiou, F., Kurz, M. & Brook, E. 1991: Examination of surface exposure ages of Antarctic moraines using *in situ*-produced ^{10}Be and ^{26}Al. *Geochimica et Cosmochimica Acta 55*, 2269–2283.

Brown, E., Bourlès, D., Colin, F., Sanfo, Z., Raisbeck, G. & Yiou, F. 1994: The Development of Iron Crust Lateritic Systems in Burkina Faso, West Africa Examined with *In Situ*-Produced Cosmogenic Nuclides - *Earth and Planetary Science Letters 124*, 19-33.

Cerdeño, E. 1998: Diversity and evolutionary trends of the Family Rhinocerotidae (Perissodactyla). *Palaeogeography, Palaeoclimatology, Palaeoecology 141*, 13–34.

Chaline, J., Laurin, B., Brunet-Lecomte, P. & Viriot, L. 1993: Morphological trends and rates of evolution in arvicolids (Arvicolidae, Rodentia): towards a punctuated equilibria/disequilibria model. *Quaternary International 19*, 27–39.

Chmeleff, J., Von Blanckenburg, F., Kossert, K. & Jakob, D. 2010: Determination of the ^{10}Be half-life by multicollector ICP-MS and liquid scintillation counting. *Nuclear Instruments and Methods in Physics Research B: Beam Interactions with Materials and Atoms 268*, 192–199.

Cordy, J.-M. 1980: Le paléokarst de la Belle-Roche (Sprimont, Liège), premier gisement paléontologique et archéologique du Pléistocène moyen ancien en Belgique. *Compte-rendu de l'Académie des Sciences de Paris, série D 291*, 749–751.

Cordy, J. M. 1982: Biozonation du Quaternaire post-villafranchien continental d'Europe occidentale à partir des grands mammifères. *Bulletin de la Société de Géologie de Belgique 105*, 303–314.

Cordy, J.-M. 1992: Apport de la paléomammologie à la paléoanthropologie en Europe. *In* Toussaint, M. *(ed.): Cinq millions d'années, l'aventure humaine – Études et recherches archéologiques de l'Université de Liège 56*, 77-94.

Cordy, J.-M. 1998: Contexte et problématique de l'industrie lithique du Paléolithique ancien de « La Belle-Roche » à Sprimont (province de Liège), *Etudes et Documents*, *Archéologie 5*, 9–22.

Cordy, J.-M. & Ulrix-Closset, M. 1981: La grotte de la Belle-Roche (Prov. de Liège, Belgique): un gisement à galets aménagés du Pléistocène moyen ancien. *Actes du X^e Congrès de l'Union Internationale des Sciences préhistoriques et protohistoriques*, Section II, 18–19. Mexico.

Cordy, J.-M. & Ulrix-Closset, M. 1991: Synthèse des dernières campagnes de sauvetage au gisement du Paléolithique inférieur de la Belle-Roche (Sprimont). *Notae Praehistoricae 10*, 3–13.

Cordy, J.-M., Bastin, B., Demaret-Fairon, M., Ek, C., Geeraerts, R., Groessens-Van Dyck, M.-C., Ozer, A., Peuchot, R., Quinif, Y., Thorez, J. & Ulrix-Closset, M. 1993: La grotte de la Belle-Roche (Sprimont, Province de Liège): un gisement paléontologique et archéologique d'exception au Benelux. *Bulletin de l'Académie royale de Belgique, Classe des Sciences*, *6ème S. 4*, 165–186.

Cornet, Y. 1995: L'encaissement des rivières ardennaises au cours du Quaternaire. *In* Demoulin, A. (ed.): *L'Ardenne, Essai de Géographie Physique*, 155–177. Département de Géographie Physique et Quaternaire, Université de Liège.

Croitor, R. & Brugal, J.-P. 2010: Ecological and evolutionary dynamics of the carnivore community in Europe during the last 3 million years. *Quaternary International 212*, 98–108.

De Moor, G. & Pissart, A. 1992: Les formes du relief. *In* Denis, J. (ed.): *Géographie de la Belgique*, 130-216. Crédit Communal, Bruxelles.

Draily, C. 1998: L'industrie lithique du Paléolithique ancien de «La Belle-Roche» à Sprimont (province de Liège). *Etudes et documents*, *Archéologie 5*, 23–56.

Draily, C. & Cordy, J.-M. 1997: L'industrie lithique de La Belle-Roche à Sprimont (Liège, Belgique) : Paléolithique inférieur. *Notae Praehistoricae 17*, 11–20.

Eisenmann, V. 1991: Les chevaux Quaternaires Européens (mammalia, perissodactyla). Taille, typologie, biostratigraphie et taxonomie. *Geobios 24*, 747–759.

Gascoyne, M. & Schwarcz, H. P. 1985: Uranium-Series dates for the lower Paleolithic site of Belle-Roche, Belgium. *Current Anthropology 26*, 641–642.

Gewelt, M. 1985: Cinétique du concrétionnement dans quelques grottes belges: apport des datations ^{14}C et $^{230}Th/^{234}U$. *Annales de la Société Géologique de Belgique 108*, 267–273.

Gosse, J. C. & Phillips, F. M. 2001: Terrestrial *in situ* cosmogenic nuclides: theory and application. *Quaternary Science Reviews 20*, 1475–1560.

Granger, D. E. & Muzikar, P. F. 2001: Dating sediment burial with *in situ* produced cosmogenic nuclides: theory, techniques, and limitations. *Earth and Planetary Science Letters 188*, 269–281.

Hidy, A. J., Gosse, J. C., Pederson, J. L., Mattern, J. P. & Finkel, R. C. 2010: A geologically constrained Monte Carlo approach to modeling exposure ages from profiles of cosmogenic nuclides: An example from Lees Ferry, Arizona. *Geochemistry, Geophysics, Geosystems 11*, 1-18.

Ivy-Ochs, S., Wüst, R., Kubik, P. W., Müller-Beck, H. & Schlüchter, C. 2001: Can we use cosmogenic isotopes to date stone artifacts? *Radiocarbon 43*, 759–764.

Juvigné, É. & Renard, F. 1992: Les terrasses de la Meuse de Liège à Maastricht. *Annales de la Société Géologique de Belgique 115*, 167–186.

Juvigné, É., Cordy, J.-M., Demoulin, A., Geeraerts, R., Hus, J. & Renson, V. 2005: Le site archéo-paléontologique de la Belle-Roche (Belgique) dans le cadre de l'évolution géomorphologique de la vallée de l'Amblève inférieure. *Geologica Belgica 8,* 121–133.

Korschinek, G., Bergmaier, A., Faestermann, T., Gerstmann, U. C., Knie, K., Rugel, G., Wallner, A., Dillmann, I., Dollinger, G., Lierse Von Gostomski, C., Kossert, K., Maiti, M., Poutivtsev, M. & Remmert, A. 2010: A new value for the half-life of ^{10}Be by Heavy-Ion Elastic Recoil Detection and liquid scintillation counting. *Nuclear Instruments and Methods in Physics Research B: Beam Interactions with Materials and Atoms 268*, 187–191.

Lal, D. 1991: Cosmic ray labeling of erosion surfaces: *in situ* nuclide production rates and erosion rates. *Earth and Planetary Science Letters 104*, 424–439.

Lisiecki, L. & Raymo, M. 2005: A Pliocene-Pleistocene stack of 57 globally distributed benthic δ^{18}O records. *Paleoceanography 20*, PA1003, doi:10.1029/2004PA001071.

Mancini, M., Cavuoto, G., Pandolfi, L., Petronio, C., Salari, L. & Sardella, R. 2012: Coupling basin infill history and mammal biochronology in a Pleistocene intramontane basin: The case of western L'Aquila basin (central Apennines, Italy). *Quaternary International 267*, 62–77.

Merchel, S. & Herpers, U. 1999: An update on radiochemical separation techniques for the determination of long-lived radionuclides via accelerator mass spectrometry. *Radiochimica Acta 84*, 215–219.

Merchel, S., Arnold, M., Aumaître, G., Benedetti, L., Bourlès, D. L., Braucher, R., Alfimov, V., Freeman, S. P. H. T., Steier, P. & Wallner, A. 2008: Towards more precise ^{10}Be and ^{36}Cl data from measurements at the 10^{-14} level: influence of sample preparation. *Nuclear Instruments and Methods in Physics Research B: Beam Interactions with Materials and Atoms 266*, 4921–4926.

Meyer, W. & Stets, J. 1998: Junge Tektonik im Rheinischen Schiefergebirge und ihre Quantifizierung. *Zeitschrift der Deutschen Geologischen Gesellschaft 149*, 359–379.

Moigne, A.-M., Palombo, M.-R., Belda, V., Heriech-Briki, D., Kacimi, S., Lacombat, F., de Lumley, M. A., Moutoussamy, J., Rivals, F., Quilès, J. & Testu, A. 2006: Les faunes de grands mammifères de la Caune de l'Arago (Tautavel) dans le cadre biochronologique des faunes du Pléistocène moyen italien. *L'Anthropologie 110*, 788–831.

Nichols, K. K., Bierman, P. R., Leb, R., Clapp, E. M. & Caffee, M. 2002: Quantifying sediment transport on desert piedmonts using ^{10}Be and ^{26}Al. *Geomorphology 45*, 105–125.

Nichols, K. K., Bierman, P. R., Eppes, M. C., Caffee, M., Finkel, R. & Larsen, J. 2005: Late Quaternary history of the Chemehuevi Mountain Piedmont, Mojave Desert, deciphered using ^{10}Be and ^{26}Al. *American Journal of Science 305*, 345–368.

Nishiizumi, K., Imamura, M., Caffee, M., Southon, J., Finkel, R. & McAninch. J. 2007: Absolute calibration of ^{10}Be AMS standards. *Nuclear Instruments and Methods in Physics Research 258*, 403-413.

Parfitt, S., Barendregt, R., Breda, M., Candy, I., Collins, M., Coope, G., Durbidge, P., Field, M., Lee, J., Lister, A., Mutch, R., Penkman, K., Preece, R., Rose, J., Stringer, C., Symmons, R., Whittaker, J., Wymer, J. & Stuart, A. 2005: The earliest record of human activity in northern Europe. *Nature 438*, 1008-1012.

Parfitt, S., Ashton, N., Lewis, S., Abel, R., Coope, R., Field, M., Gale, R., Hoare, P., Larkin, N., Lewis, M., Karloukovski, V., Maher, B., Peglar, S., Preece, R., Whittaker, J. & Stringer, C. 2010: Early Pleistocene human occupation at the edge of the boreal zone in northwest Europe. *Nature 466*, 229-233.

Partridge, T. C., Granger, D., Caffee, M. W. & Clarke, R. J. 2003: Lower Pliocene hominid remains from Sterkfontein. *Science 300*, 607–612.

Pissart, A. 1995: L'Ardenne sous le joug du froid – Le modelé périglaciaire du massif ardennais. *In* Demoulin, A. (ed.): *L'Ardenne, Essai de Géographie Physique*, 136–154. Département de Géographie Physique et Quaternaire, Université de Liège.

Renson, V., Juvigné, E. & Cordy, J.-M. 1997: L'Homme était-il présent en haute Belgique il y a un million d'années ? *Notae Praehistoricae 17*, 7–9.

Renson, V., Juvigné, E. & Cordy, J.-M. 1999: Découverte en faveur d'une révision de la chronologie du Quaternaire : la grotte de la Belle-Roche (Belgique); hypothèse nouvelle concernant l'ancienneté de l'Homme en Europe du nord-ouest. *Compte-rendu de l'Académie des Sciences de Paris (Sciences de la Terre et des Planètes) 328*, 635–640.

Rixhon, G. & Demoulin, A. 2010: Fluvial terraces of the Amblève: a marker of the Quaternary river incision in the NE Ardenne massif (western Europe). *Zeitschrift für Geomorphologie 54*, 161–180.

Rixhon, G. & Juvigné, É. 2010: Periglacial deposits and correlated processes in the Ninglinspo valley (Ardenne massif, Belgium). *Geologica Belgica 13*, 49-60.

Rixhon, G., Braucher, R., Bourlès, D., Siame, L., Bovy, B. & Demoulin, A. 2011: Quaternary river incision in NE Ardennes (Belgium) – Insights from ^{10}Be/^{26}Al dating of river terraces. *Quaternary Geochronology 6*, 273–284.

Siame, L., Bellier, O., Braucher, R., Sébrier, M., Cushing, M., Bourlès, D., Hamelin, B., Baroux, E., De Voogd, B., Raisbeck, G. & Yiou, F. 2004: Local erosion rates versus active tectonics: cosmic ray exposure modeling in Provence (south-east France). *Earth and Planetary Science Letters 220*, 345–364.

Stone, J.O. 2000: Air pressure and cosmogenic isotope production. *Journal of Geophysical Research 105*, 23753–23759.

Van Balen, R., Houtgast, R., Van der Wateren, F., Vandenberghe, J. & Bogaart, P. 2000: Sediment budget and tectonic evolution of the Meuse catchment in the Ardennes and the Roer valley Rift system. *Global & Planetary Change 27*, 113–129.

Van den Berg, M. 1996: *Fluvial sequences of the Maas, a 10 Ma record of neotectonics and climate change at various timescales.* Ph.D. thesis, Universiteit Wageningen, 181 pp.

Vandenberghe, J. 1995: Timescales, climate and river development. *Quaternary Science Reviews 14*, 631–638.

Van der Made, J. 2001: Les ongulés d'Atapuerca. Stratigraphie et biogéographie. *L'Anthropologie 105*, 95–113.

Vermeesch, P. 2007: CosmoCalc: an Excel add-in for cosmogenic nuclide calculations. *Geochemistry, Geophysics, and Geosystems 8*. doi:10.1029/2006GC001530 Q08003.

Verri, G., Barkai, R., Bordeanu, C., Gopher, A., Hass, M., Kaufman, M., Kubik, P. W., Montanari, E., Paul M., Ronen, A., Weiner, S. & Boaretto, E. 2004: Flint mining in prehistory recorded by *in situ*-produced cosmogenic ^{10}Be. *Proceedings of the National Academy of Sciences 101*, 7880–7884.

Verri, G., Barkai, R., Gopher, A., Hass, M., Kubik, P. W., Paul, M., Ronen, A., Weiner, S. & Boaretto E. 2005: Flint procurement strategies in the Late Lower Palaeolithic recorded by *in situ*-produced cosmogenic ^{10}Be in Tabun and Qesem Caves (Israel). *Journal of Archaeological Science 32*, 207–213.

Table caption

Table 1. Results of the ^{10}Be analysis and concentration measurements. Shielding factor is equal to 1 for the Belle-Roche terrace; the elevation refers to the top of the alluvial deposits at the sample site.

Figure captions

Fig. 1. A. Location of the study area (black dot) at the northern margin of the Ardennes massif, NW Europe. ECRS = European Cenozoic Rift System. B. Location of the Belle-Roche site (black rectangle) in eastern Belgium. C. Simplified geological map of the lower reach of the Amblève valley with the Belle-Roche site. D. Simplified N–S geological cross section in the lower Amblève valley. The Belle-Roche palaeokarst and terrace (B-R T) are both cut into the northern limb of a limestone syncline and are respectively located at relative elevations of ~57 m and ~53 m (terrace top) above the top of the current floodplain (FP). The sediment thickness in the latter is 5 m at the confluence with the Ourthe River (2 km downstream). HT refers to a higher (older) terrace level of the Amblève and the dotted line defines the approximate shape of the valley at the Pliocene/Pleistocene boundary (see Rixhon & Demoulin 2010). The black rectangle refers to the cross section of the Belle-Roche terrace in Fig. 5A.

Fig. 2. A. Schematic block-diagram of the Belle-Roche palaeokarst showing galleries (numbered from I to IV) orientation and associated shafts (modified from Cordy *et al.* 1993). B. General view of the infill deposits in gallery IV. River sediments of the Amblève lie on the limestone bedrock at the base of the palaeocave; their thickness reaches ~1 m in the palaeo-channel (P-Ch) visible in the lower right of the picture. A complex of slope deposits (run off and solifluction products) with archaeological and

palaeontological remains (see text) overlie this alluvium and may be up to 3 m thick. C. Detailed view of the slope deposit complex characterized by a normal polarity and sealed by a flowstone dated >350 ka by U/Th (Gascoyne & Schwarcz 1985).

Fig. 3. Bone remains of four big carnivore species (A, C, D, E), one herbivore species (B) and one rodent species (F) found in the slope deposits. A. *Canis mosbachensis* (jowl). B. *Hemitragus bonali* (jowl). C. *Panthera onca gombaszoegensis* (skull). D. *Panthera leo fossilis* (jowl). E. *Ursus deningeri* (skull). F. *Arvicola cantiana* (skull). All photos by J.-M. Cordy.

Fig. 4. Traces of past human presence at the Belle-Roche site (mostly artefacts), included within the uppermost filling layer of the palaeokarst. A. Transverse and convex flint scraper. B. Flint chopping tool. C. Flint biface. D. Metapodium of *Ursus Deningeri* with deep, angular notches (shown by the white arrows) resulting from man activity (e.g. skin or flesh removal). All photos and drawings by J.-M. Cordy.

Fig. 5. A. Cross section in the eastern part of the Belle-Roche terrace (YMT) (modified from Juvigné *et al.* 2005) with location of our trenches (T1, corresponding to the ^{10}Be sampling profile, and T2) and the trenches made by Juvigné *et al.* (2005) (J1 to 4). Seismic sounding shows that the alluvial sediments are about 8 m thick at the sampling locality. The base and top of the terrace sediments are respectively located at ~145 and ~154 m a.s.l. while colluvial deposits cap the marginal part of the terrace (T2). At this place, the limestone bedrock was reached at a depth of 3.7 m. The palaeokarst insert indicates the altitudinal relationship between cave filling and terrace. B. Section at the sampling place. A' = modern soil; B' = fluvial gravel made of pebbles and cobbles embedded within a fine matrix. Be07-BR20 to Be07-BR29 labels refer to the ^{10}Be samples and indicate their respective sampling depth.

Fig. 6. A. ^{10}Be depth profile (expressed both in cm and g cm^{-2}) of the Belle-Roche terrace with the measured concentrations (squares) and their analytical uncertainties (error bars). The concentration values obviously pertain to distinct ^{10}Be profiles in the upper and lower halves of the deposit and consequently require a two-step treatment. B. Modelling of the exposure time (single cosmic ray

exposure episode) based on the five upper samples (the bold curve represents the modelled concentrations), yielding an age of 222.5±31 ka for the abandonment time of the terrace. C. Modelling step aimed at matching the specific cosmogenic signal below 3 m depth (dashed curve). This curve integrates the initial slow burial of the fluvial sediments and their subsequent ~222.5 ka exposure time after terrace abandonment.

Fig. 7. Relationship between palaeomagnetism, the ^{10}Be dating of the Belle-Roche terrace (onset of terrace formation and abandonment time), the Marine Isotopic Stages, and the biozones of 20 representative mammal species found in the palaeokarst filling. Based on the ^{10}Be dating of the terrace, the shaded rectangle in the right half of the diagram indicates the time range during which the whole filling of the palaeokarst occurred (deposition of the fluvial gravel first and of the fossil-bearing layers afterwards). All data are consistent with attribution of the faunal remains to MIS 14–13 (darker area in the shaded rectangle), although they might also pertain to MIS 12–11 (see text).

Sample	Latitude (°N)	Longitude (°E)	Elevation (m a.s.l.)	Depth (cm)	Depth (g cm^{-2})	Stone scaling factor [1] (at g^{-1} a^{-1})	Dissolved quartz (g)	^{9}Be Carrier [2] (10^{19} at)	^{10}Be/^{9}Be	^{10}Be (10^{5} at g^{-1})	^{10}Be error (10^{5} at g^{-1})
Be07 BR-20				600	1380		46,641	2,040	4.15E-13	1,815	0.037
Be07 BR-21				550	1265		45,645	2,051	2.42E-13	1,087	0.031
Be07 BR-22				500	1150		43,727	2,040	3.32E-13	1,548	0.037
Be07 BR-23				450	1035		44,363	2,043	2.47E-13	1,137	0.033
Be07 BR-24	50,481	5,616	153	400	920	1,180	45,887	2,046	1.56E-13	0.695	0.022
Be07 BR-25				300	690		44,548	2,048	1.12E-13	0.514	0.019
Be07 BR-26				200	460		46,079	2,041	1.63E-13	0.722	0.025
Be07 BR-27				150	345		43,691	2,078	3.00E-13	1,429	0.031
Be07 BR-28				100	230		41,630	2,011	4.41E-13	2,131	0.037
Be07 BR-29				60	138		42,690	2,050	7.50E-13	3,600	0.061

[1] Production rate was scaled with a sea level high latitude production rate of 4.5±0.3 at g^{-1} a^{-1}.

[2] For each sample, addition of ~100 µl of an in-house 3.10^{-3} g g^{-1} ^{9}Be carrier solution (deep-mined phenakyte crystal).

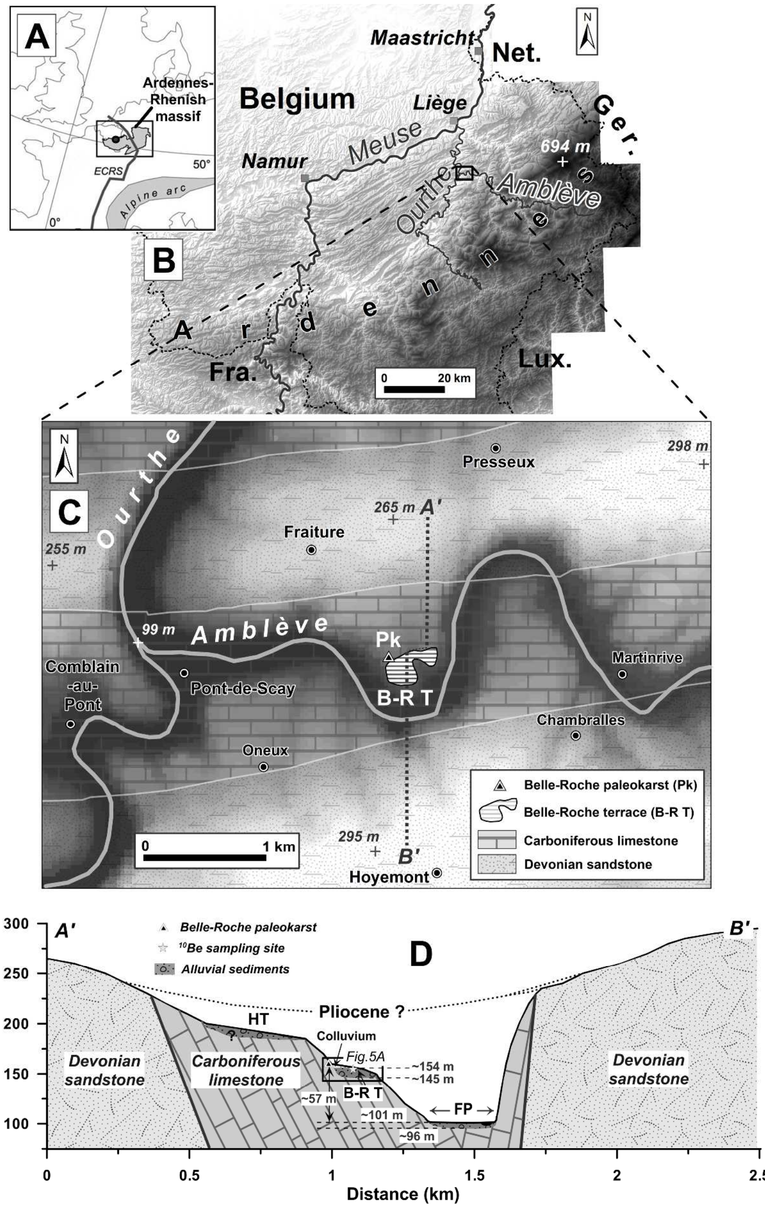
A
Ardennes-Rhenish massif
50°
ECRS
Alpine arc
0°
B
Maastricht
Net.
Belgium
Liège
Ger.
Namur
Meuse
694 m
Ourthe
Amblève
A r d e n n e s
Fra.
Lux.
0
20 km
C
Ourthe
Presseux
298 m
265 m
A'
Fraiture
255 m
99 m
Amblève
Pk
B-R T
Comblain-au-Pont
Pont-de-Scay
Martinrive
Chambralles
Oneux
0
1 km
295 m
B'
Hoyemont
Belle-Roche paleokarst (Pk)
Belle-Roche terrace (B-R T)
Carboniferous limestone
Devonian sandstone
D
A'
B'
Belle-Roche paleokarst
10Be sampling site
Alluvial sediments
Pliocene ?
HT
Colluvium
Fig.5A
~154 m
~145 m
B-R T
~57 m
~101 m
~96 m
FP
Devonian sandstone
Carboniferous limestone
Devonian sandstone
Elevation (m a.s.l.)
300
250
200
150
100
0
0.5
1
1.5
2
2.5
Distance (km)

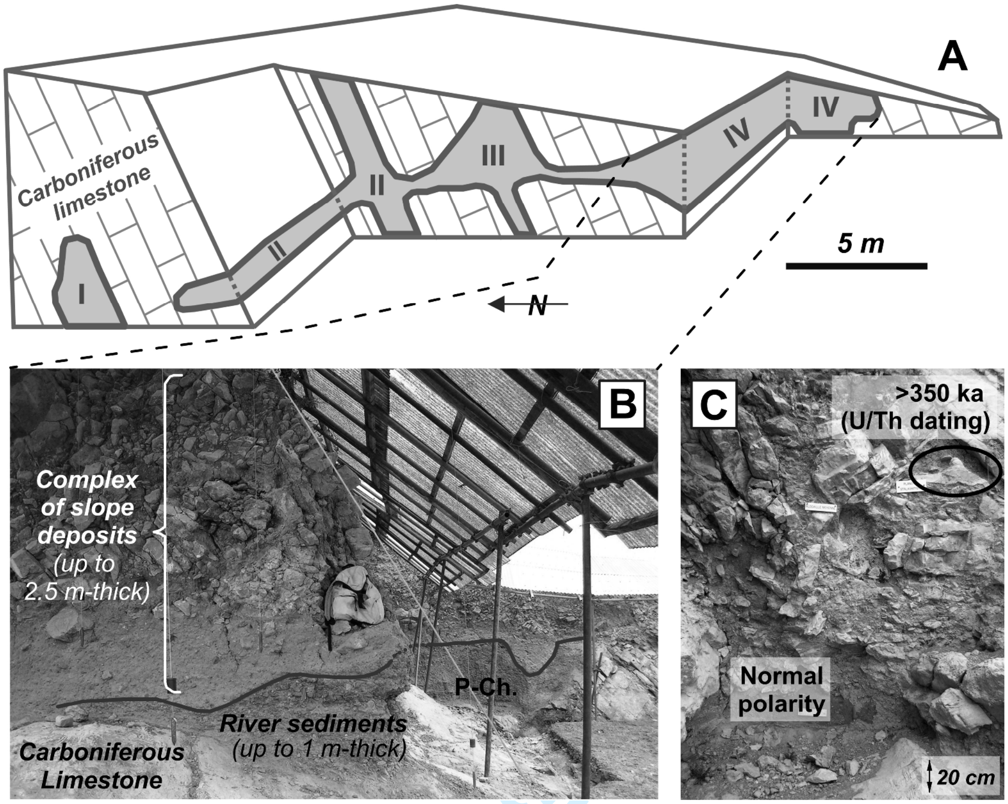
A
Carboniferous limestone
I
II
III
IV
5 m
N
B
Complex of slope deposits (up to 2.5 m-thick)
P-Ch.
River sediments (up to 1 m-thick)
Carboniferous Limestone
C
>350 ka (U/Th dating)
Normal polarity
20 cm

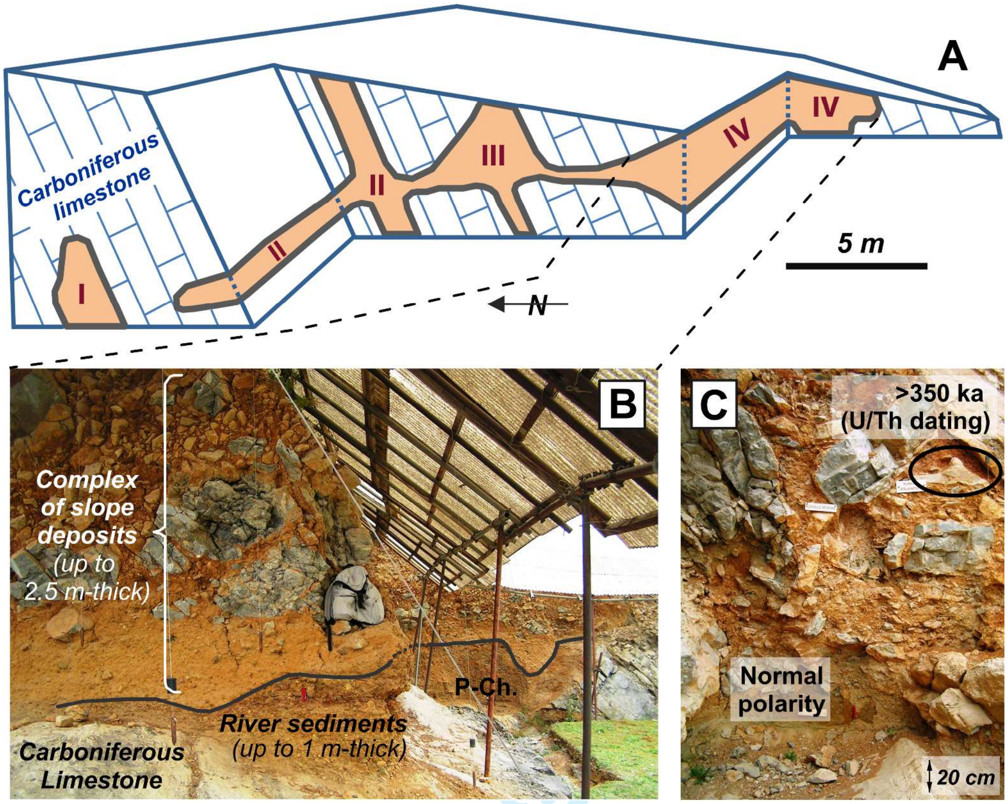
A
Carboniferous limestone
I
II
II
III
IV
IV
5 m
N
B
Complex of slope deposits (up to 2.5 m-thick)
P-Ch.
River sediments (up to 1 m-thick)
Carboniferous Limestone
C
>350 ka (U/Th dating)
Normal polarity
20 cm

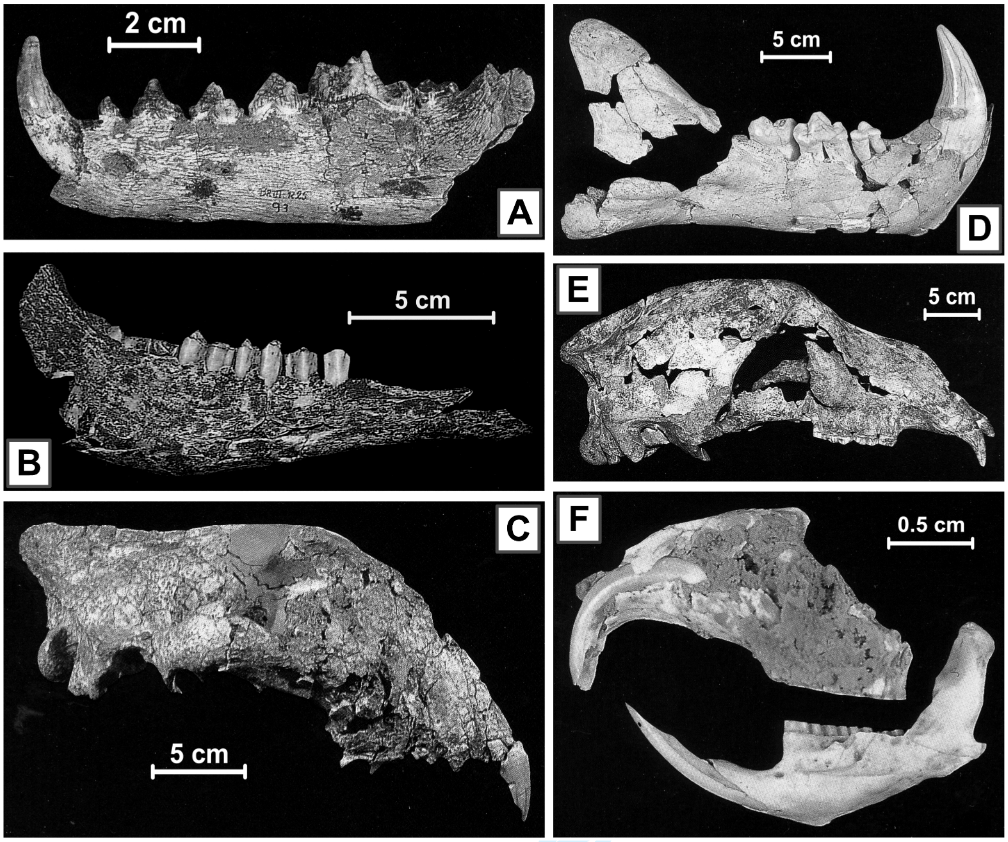
2 cm
A
D
5 cm
5 cm
B
E
5 cm
C
F
0.5 cm
5 cm

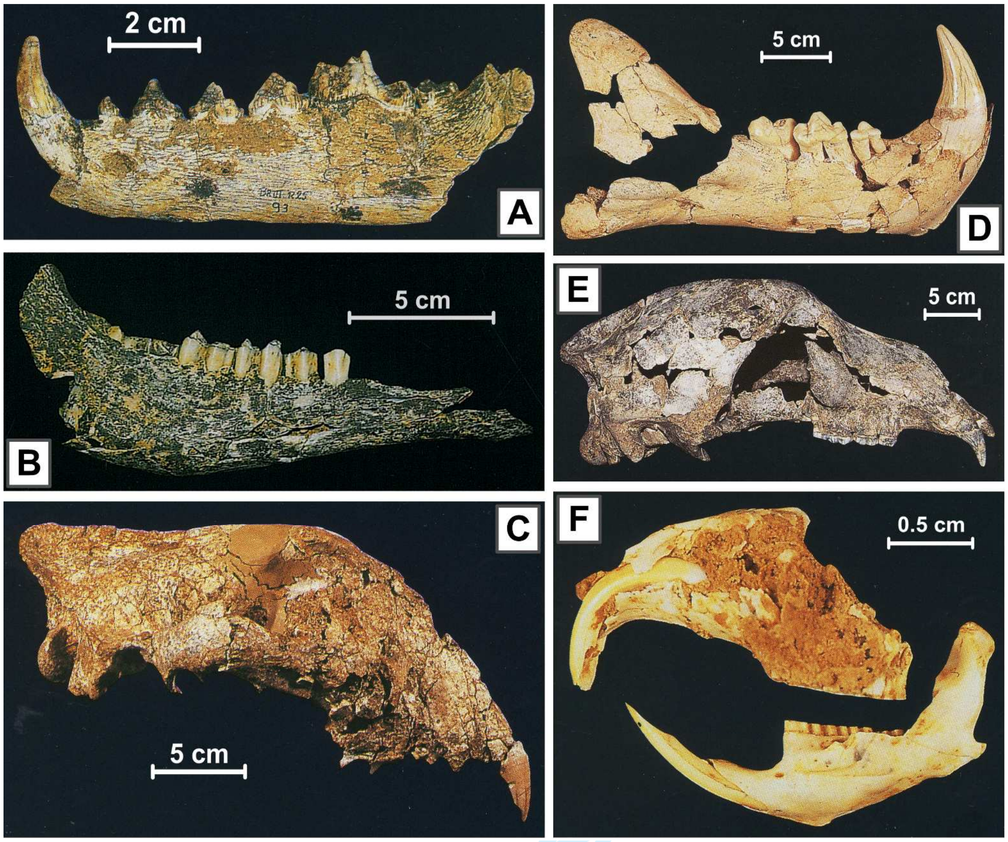
2 cm
A
5 cm
D
5 cm
B
E
5 cm
C
F
0.5 cm
5 cm

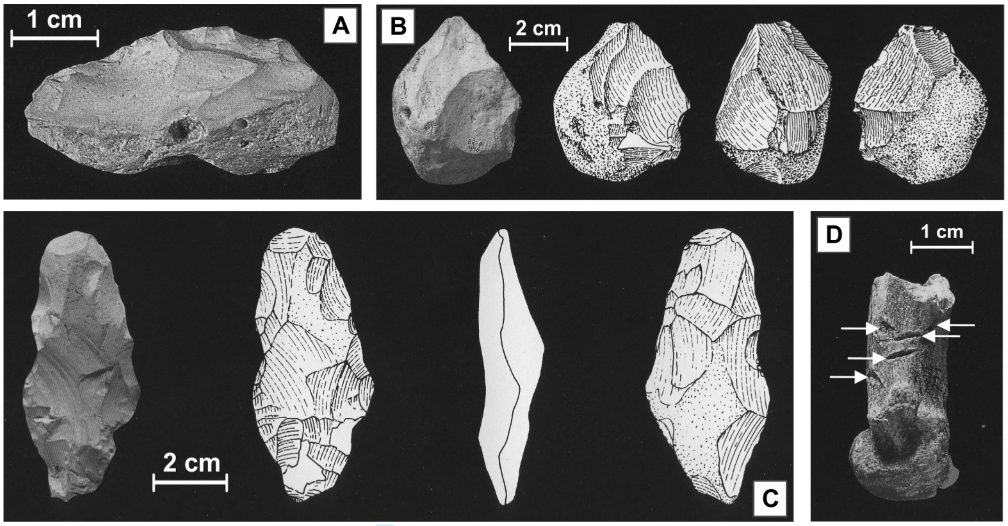
1 cm
A
B
2 cm
2 cm
C
D
1 cm

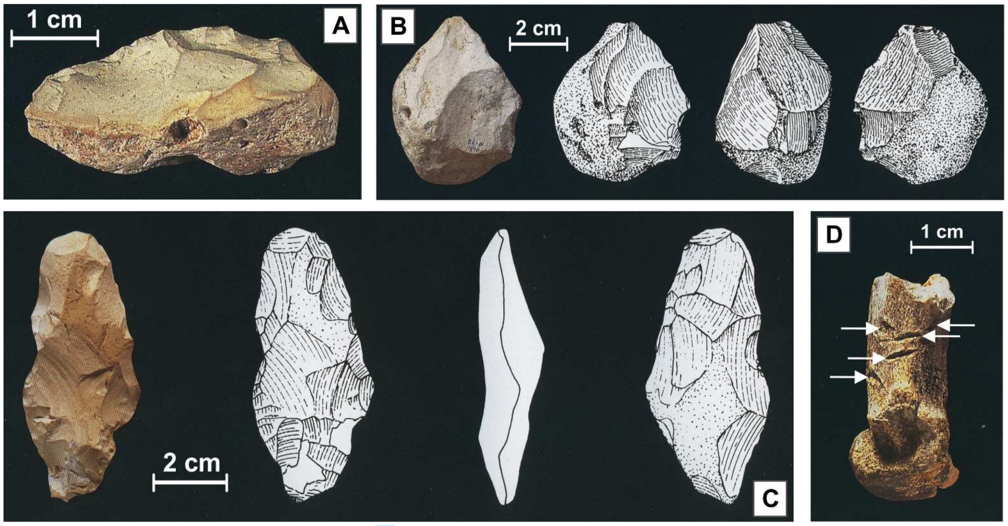
1 cm
A
B
2 cm
2 cm
C
D
1 cm

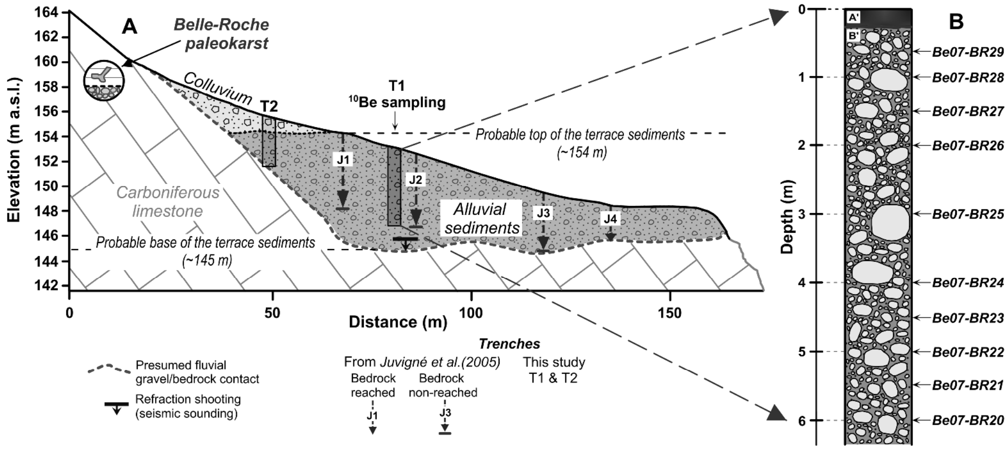
A
B
Belle-Roche paleokarst
Colluvium
T2
T1
^{10}Be sampling
Probable top of the terrace sediments (~154 m)
Carboniferous limestone
Alluvial sediments
Probable base of the terrace sediments (~145 m)
J1
J2
J3
J4
Elevation (m a.s.l.)
Distance (m)
Depth (m)
Presumed fluvial gravel/bedrock contact
Refraction shooting (seismic sounding)
Trenches
From Juvigné et al.(2005)
Bedrock reached
Bedrock non-reached
This study T1 & T2
A'
B'
Be07-BR29
Be07-BR28
Be07-BR27
Be07-BR26
Be07-BR25
Be07-BR24
Be07-BR23
Be07-BR22
Be07-BR21
Be07-BR20

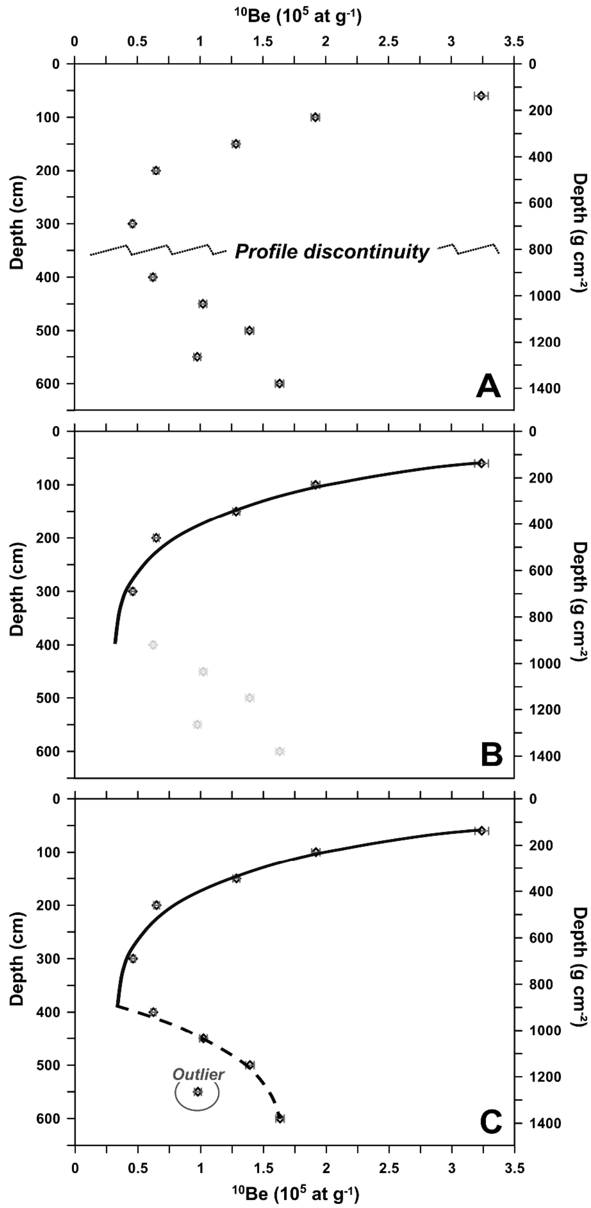

10Be (10^5 at g-1)
Depth (cm)
Depth (g cm-2)
Profile discontinuity
Outlier
A
B
C

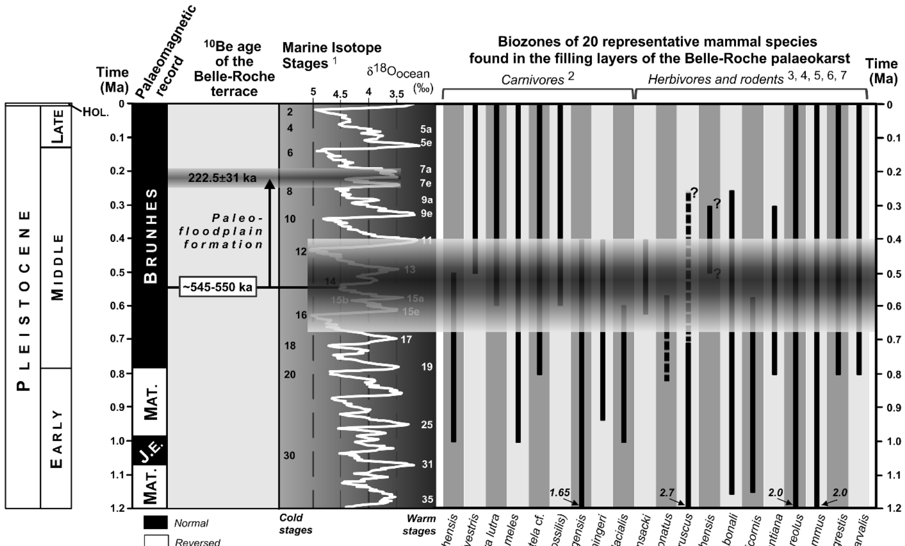

[1] MIS curve from the *International Commission on Stratigraphy* (http://www.stratigraphy.org/upload/QuaternaryChart.pdf) and constructed from a stack of 57 globally distributed benthic $\delta^{18}O$ records
[2] data from Croitor & Brugal (2010)
[3] data from Eisenmann (1991)
[4] data from Chaline *et al.* (1993)
[5] data from Cerdeño (1998)
[6] data from Van der Made (2001)
[7] data from Mancini *et al.* (2012)